THE ASTROPHYSICAL JOURNAL, 301:27–34, 1986 February 1

CONTRACTION OF DARK MATTER GALACTIC HALOS DUE TO BARYONIC INFALL[1]

GEORGE R. BLUMENTHAL AND S. M. FABER
Lick Observatory, Board of Studies in Astronomy and Astrophysics, University of California, Santa Cruz

RICARDO FLORES
Department of Physics, Brandeis University, Waltham, Massachusetts

AND

JOEL R. PRIMACK
Board of Studies in Physics, University of California, Santa Cruz
Received 1985 June 14; accepted 1985 July 9

ABSTRACT

Varied evidence suggests that galaxies consist of roughly 10% baryonic matter by mass and that baryons sink dissipatively by about a factor of 10 in radius during galaxy formation. We show that such infall strongly perturbs the underlying dark matter distribution, pulling it inward and creating cores that are considerably smaller and denser than would have evolved without dissipation. Any discontinuity between the baryonic and dark matter mass distributions is smoothed out by the coupled motions of the two components. If dark halos have large core radii in the absence of dissipation, the above infall scenario yields rotation curves that are flat over large distances, in agreement with observations of spiral galaxies. Such large dissipationless cores may plausibly result from large internal kinetic energy in protogalaxies at maximum expansion, perhaps as a result of subclustering, tidal effects, or anisotropic collapse.

Subject headings: galaxies: evolution — galaxies: internal motions — galaxies: structure — interstellar: matter

I. INTRODUCTION

The remarkably flat rotation curves of spiral galaxies (e.g., Bosma 1978; Rubin, Ford, and Thonnard 1980; Rubin 1982) demand explanation in any theory of galaxy formation. There are at least two aspects to be considered: flatness at large distances beyond the optical radius, which implies the existence of large, dark halos with density falling approximately as r^{-2}; and flatness at small distances, where the disk mass is gravitationally important. The observed smooth transition between the two suggests the existence of a physical mechanism which is responsible for the continuity between the mass densities of the disk and halo (Burstein and Rubin 1985; Bahcall and Casertano 1985).

Although complete violent relaxation of an unbounded region produces an isothermal sphere with $\rho \propto r^{-2}$ (Lynden-Bell 1967; Shu 1978), N-body simulations of collapsing spherically symmetric homogeneous "top-hat" fluctuations lead to density profiles that typically fall off as $r^{-3.5}$ (Gott 1973). Secondary infall of matter surrounding the perturbation can lead to density profiles that are less steep at large distances (Gunn and Gott 1972; Gott 1975; Gunn 1977). This was confirmed by N-body simulations of a region surrounding a central mass point containing $\sim 10\%$ of the total mass (Dekel, Kowitt, and Shaham 1981), although other work (Pryor and Lecar 1983) disagrees, possibly because the collapses there were unrealistically constrained to be spherical. Recent related work has been done by Smith and Miller (1985).

In this paper we consider the origin of flat rotation curves in a model of galaxy formation based on gravitational collapse of a protogalaxy containing a homogeneous mixture of dissipationless dark matter and roughly 10% baryonic material (White and Rees 1978; Faber 1982; Gunn 1982; Blumenthal *et al.* 1984). Although galaxy mass models (Caldwell and Ostriker 1982; Bahcall, Schmidt, and Soneira 1982) distinguish between dissipative and dissipationless components, most previous work on galaxy formation has treated the dissipationless halo as "rigid" (e.g., Fall and Efstathiou 1980). Here we explicitly consider the gravitational response of the halo to the dissipative baryonic infall. The next section treats this problem using a simple analytic model and concludes that baryonic infall can indeed produce rotation curves comparable to those observed starting from an isothermal sphere with a large core radius. Section III describes a crude first attempt at N-body simulations to model baryonic dissipation. Section IV discusses the results in light of recent speculations on the origin of flat rotation curves, and § V summarizes our conclusions.

II. ANALYTIC MODELS

The response of a dissipationless halo to the infall of a small dissipational fraction of its mass can be conveniently described using an approximate analytic model. This model uses the fact that, for periodic orbits, $\oint pdq$ is an adiabatic invariant, where p is the conjugate momentum of the coordinate q. If p represents the angular momentum of a particle in a circular orbit within some spherically symmetric mass distribution $M(r)$, then $rM(r)$ is constant for that particle so long as the mass internal to its orbit changes slowly with time (Steigman *et al.* 1978; Zeldovich *et al.* 1980; Ryden and Gunn 1984). For purely radial orbits, it is easy to show that the quantity $r_{\max} M(r_{\max})$ is also constant if $M(r)$ varies in a self-similar fashion. Since there is more phase space available for nearly circular orbits than for radial orbits, we make the simplifying approximation that the orbits of dissipationless halo particles are circular. Furthermore, if the initial fraction of dissipational baryonic mass $F \equiv M_b/M \ll 1$, the mass interior to a dissipationless particle's orbit will not show a large fractional change during one orbital period even if dissipation occurs rapidly, provided the particle is fairly far from the galaxy

[1] *Lick Observatory Bulletin*, No. 1017.

center. This assures that the orbits of all but the innermost halo particles change adiabatically.

Assume that the initial spherically symmetric mass distribution of the galaxy $M_i(r)$ represents a dynamical equilibrium state with a constant fraction F of dissipational baryons as a function of r. The dissipational particles will then cool and fall into a final mass distribution $M_b(r)$, which, in the case of a spiral galaxy, is constrained by the initial angular momentum distribution. The adiabatic invariant of the dissipationless particle orbits implies

$$r[M_b(r) + M_x(r)] = r_i M_i(r_i) = r_i M_x(r)/(1 - F) , \qquad (1)$$

which can be solved iteratively for the final dark-matter mass distribution $M_x(r)$ given the initial total mass distribution $M_i(r_i)$ and the final baryon mass distribution $M_b(r)$. Here r_i is the initial orbital radius, and $M_x(r) = (1 - F)M_i(r_i)$, because by assumption dissipationless particle orbits do not cross. We take the initial mass distribution $M_i(r_i)$ to be an isothermal gas sphere with a core radius $a_{\rm core} = 3\sigma/(4\pi G\rho_0)^{1/2}$, where ρ_0 is the central density and σ is the one-dimensional rms velocity dispersion. The final baryonic mass distribution is assumed to be of the form $M_b(r) \propto 1 - (1 + r/b) \exp(-r/b)$, which describes the radial mass distribution of a thin disk whose density in the plane of the disk decreases exponentially with scale length b.

Figure 1 shows the rotation curves for various values of F and b resulting from dissipation within an initial isothermal sphere whose core radius a is 42% of its outer (truncated) radius. We assume there is no baryonic infall and therefore no change in the dissipationless matter beyond $r = 1$. The figure shows that for $F = 0.1$ and $b = 0.07$, the rotation curve is rather flat beyond a couple of disk scale lengths, even though the initial rotation curve is not flat. Figure 1 also demonstrates the sensitivity of the resulting rotation curves to the dissipational mass fraction F and the disk scale length b. For F substantially greater than 0.1, the rotation curve declines after about two disk scale lengths, while for very small F, dissipation produces too little change in the rotation curve. This choice of initial core radius and b then requires $0.05 < F < 0.2$ to reproduce observed rotation curves. The final rotation curve is also sensitive to the amount of dissipational infall. For very small b, the large central mass concentration of both dissipationless and dissipational particles leads to a peaked rotation curve, whereas, for too little infall, the rotation curve rises monotonically. The amount of dissipational infall producing a flat rotation curve corresponding to $b = 0.07$ is comparable to the amount of baryonic infall implied by the tidal torque theory of galaxy angular momentum for disks with heavy halos (Fall and Efstathiou 1980).

Using the solution to equation (1) for $M_x(r)$ and for the relation between the initial and final disspationless particle radius, it is straightforward to solve for the radial dependence of the density

$$\rho(r) = [M_b'(r) + M_x'(r)]/4\pi r^2 , \qquad (2)$$

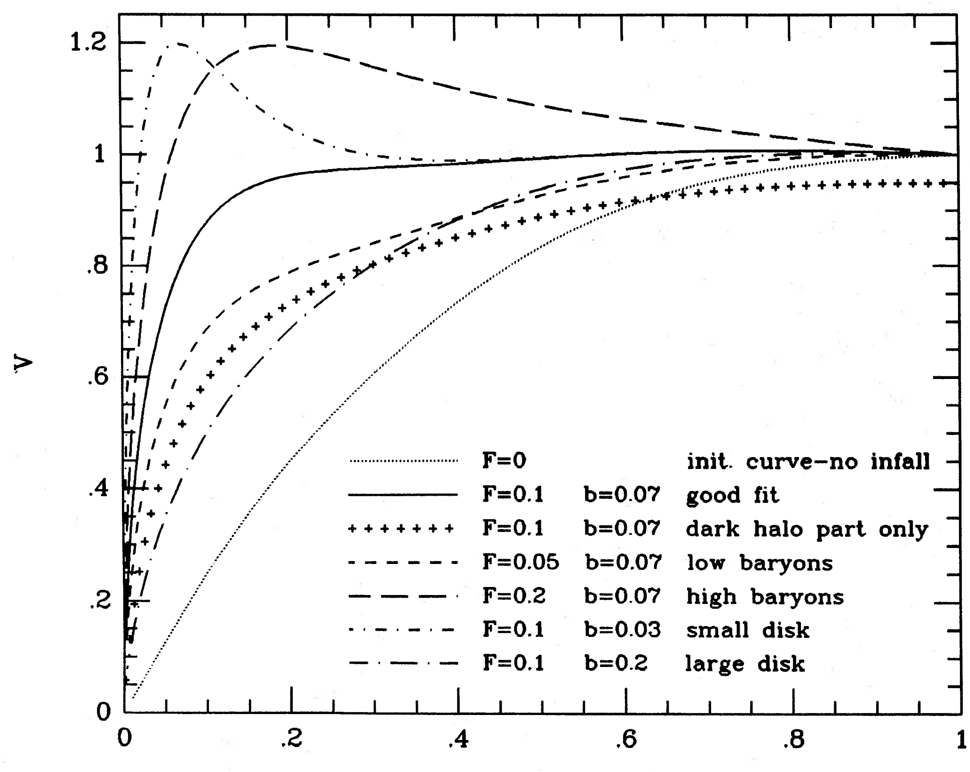

FIG. 1.—A plot of the rotational velocity, $v = (M/r)^{1/2}$, vs. r for the adiabatic invariant result given in eq. (1). The curves assume an initial isothermal gas sphere with core radius $a_{\rm core} = 0.42$. The baryonic fraction F is assumed to dissipate and fall into an exponential disk with scale length b. No dissipation is assumed to occur beyond $r = 1$. All curves except the plusses correspond to total rotational velocity; the curve denoted by plus signs is the rotational velocity due to the dissipationless particles alone for the case where $F = 0.1$ and $b = 0.07$.

where

$$M_x'(r) = \frac{(1-F)[M_b(r) + rM_b'(r) + M_x(r)]}{r_i - r(1-F) + M_i(r_i)/M_i'(r_i)}, \tag{3}$$

and where the prime denotes differentiation. Figure 2 shows a plot of the density distributions, assumed spherical, that correspond to the rotation curves in Figure 1. The figure shows that substantial changes in the density of dissipationless particles occur within a few exponential scale heights of the baryons. In fact, after dissipation, the distribution of dissipationless particles no longer resembles an isothermal sphere but is instead much more centrally peaked. For the case $F = 0.1$ and $b = 0.07$, which gives a flat rotation curve, the densities of dissipational baryons and dissipationless particles are about equal at $r = b$.

An important feature of Figures 1 and 2 is that the final "effective core radius" of the dissipationless halo particles is significantly smaller than the initial core radius a because of the effects of baryonic dissipation. For initial core radii somewhat larger than the value $a = 0.42$ used in Figure 1, it is still possible to obtain acceptable rotation curves for reasonable values of F and b. However, we find that much smaller initial core radii lead to peaked rotation curves if F is close to 0.1 and b is about 0.07. The issue of how to determine an appropriate value for the initial core radius is discussed further in the following section.

III. N-BODY SIMULATIONS

The analytic models just described are based on the use of an adiabatic invariant that assumes circular or purely radial orbits, spherical symmetry, and an equilibrium starting point. These assumptions can be relaxed and more general cases can be investigated using N-body techniques.

a) Methods

N-body simulations were carried out using the NBODY2 code developed by S. J. Aarseth (1979) using the Ahmad-Cohen scheme for the different treatment of the force due to nearby and distant particles. Particles interact via a softened potential

$$\phi_{ij} = -Gm_i m_j/(r_{ij}^4 + \epsilon^4)^{1/4}, \tag{4}$$

where the subscripts i, j refer to particles and ϵ is the softening parameter which suppresses two-body relaxation effects. The potential in equation (4) differs from the more familiar softening expression of the form $(r^2 + \epsilon^2)^{1/2}$; it was introduced to more accurately model the gravitational potential down to the effective radius ϵ of the particles while still effectively suppressing large velocity changes in two-body encounters. Integration time steps were chosen so that the fractional change in the total energy $\Delta E/E < 0.01$. The integration continued until several dynamical times after the system reached approximate equilibrium, usually 10–12 dynamical times in all; and the values of

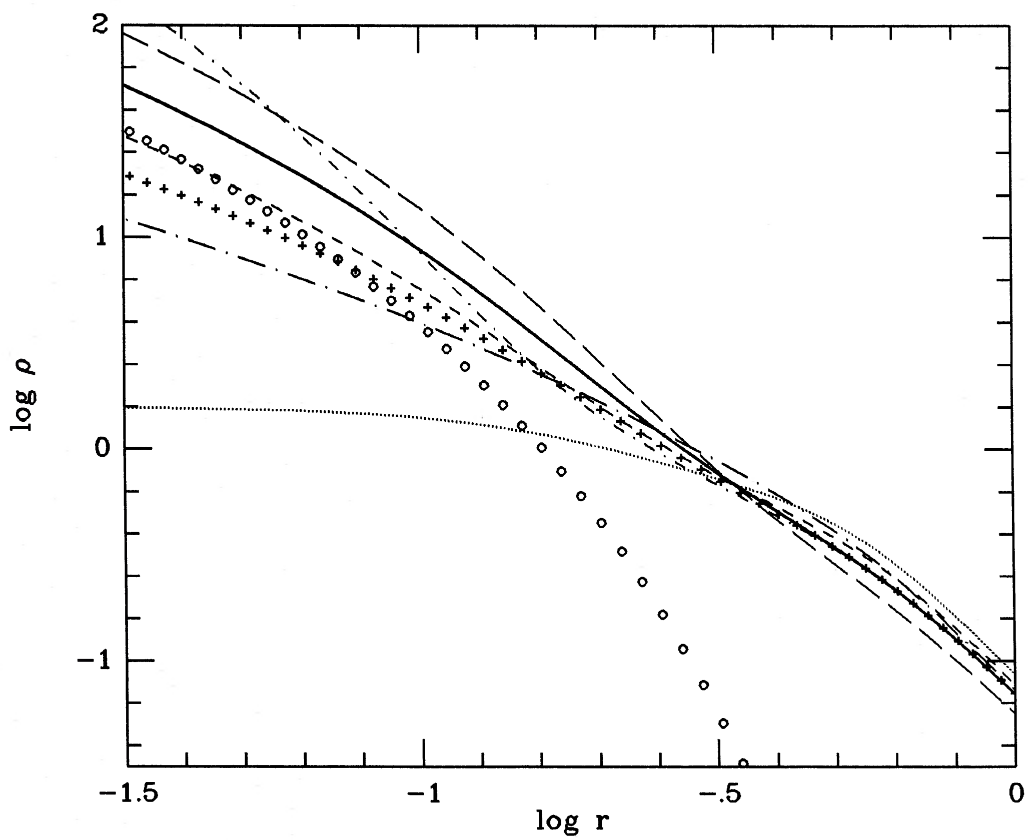

FIG. 2.—A plot of the density ρ vs. radius r for the adiabatic invariant result given in eq. (2). The cases plotted are identical with Fig. 1, and symbols are as in Fig. 1. The open circles show the dissipational baryonic density for the case $F = 0.1$ and $b = 0.07$. The density is normalized so that $M(1) = 1$; this corresponds to an initial central density $\rho(0) = 1.58$.

quantities discussed below such as $M(r)$ were obtained by averaging over the last several dynamical times.

The system was chosen to have total mass $M = 1.0 \times 10^{12}$ $M_{\odot}$, consisting of 500 dissipationless particles (the dark matter) and 500 dissipational particles (the baryons). The baryons typically constituted 10% of the total mass, so that the dark matter consisted of 500 clouds of mass $m_x = 1.8 \times 10^9$ $M_{\odot}$ each, and the baryonic matter initially consisted of 500 clouds of mass $m_b = 0.2 \times 10^9$ $M_{\odot}$; however, we also ran simulations with different percentages of dissipational material.

The key feature of the simulations is the dissipational material that we identify with baryons. In all simulations, the baryonic particles were initially mixed uniformly with the dark matter particles. In dissipational simulations, baryonic particles were given a collisional cross section σ, which was kept constant throughout a simulation. A collision occurred if two particles i, j came within distance $|\boldsymbol{r}_i - \boldsymbol{r}_j| = (\sigma/\pi)^{1/2}$ of each other, in which case they merged to form a single particle with mass $m = m_i + m_j$ located at the center of mass (CM) of the two particles and moving with the CM velocity. Their relative energy was thus dissipated. Total angular momentum should be conserved with such a scheme, and it is found to have a fractional change $\delta J/J < 0.01$. (Particle merging has been treated previously in the context of N-body simulations by Jones and Efstathiou 1979 and Aarseth and Fall 1980, who modeled galaxy mergers.)

The cross section σ is a tunable parameter that controls the rate at which baryonic material falls into the center; for larger σ, the baryons fall in faster. We chose σ so that the total energy loss rate per unit volume for a system of baryonic particles with number density n_b and a Maxwellian distribution of velocities equals the physical cooling rate (assuming fully ionized H + He):

$$dE/dtdV = n_b^2 \sigma \langle |\boldsymbol{v}_i - \boldsymbol{v}_j| \delta E_{ij} \rangle = n_p^2 \Lambda(T) , \qquad (5)$$

where n_p is the proton number density, $\Lambda(T)$ is the cooling rate (Gould and Thakur 1970), $|\boldsymbol{v}_i - \boldsymbol{v}_j|$ is the relative speed of the two particles, δE_{ij} is the energy lost in the inelastic collision, and the average is taken over a Maxwellian distribution of velocities. We find that

$$\sigma \approx \pi (3.6 \text{ kpc})^2 \left(\frac{m_b}{0.2 \times 10^9 \ M_{\odot}} \right) \left(\frac{\Lambda(T)}{10^{-23} \text{ cm}^3 \text{ ergs s}^{-1}} \right) \times \left(\frac{T}{10^6 \text{ K}} \right)^{-3/2} . \qquad (6)$$

The scaling of σ with m_b was tested by running two identical simulations that differed only in that one had twice the number of baryons of half the mass and half the cross section σ. We found no difference except for a few evolutionary details.

This treatment of dissipation is of course very crude. For one thing, the cross sectional radius is a large fraction of the scale size of the system, especially in the inner parts of the galaxy. In future, one might wish to allow σ some radial or ambient density dependence, to dissipate in some other way without merging, to terminate dissipation when baryonic density reaches the threshold for star formation, or to include shock and pressure effects on the motion of the baryons.

b) N-Body Results

The remainder of this section discusses three sets of N-body simulations: (*a*) "cold start" models, involving infall of a homogeneous sphere from rest with dissipation; (*b*) "hot start" models, in which infall starts from a uniform-density sphere in both position and velocity space with the virial condition $Q \equiv KE/|PE| = 0.5$ satisfied; and (*c*) "Hubble start" models, based on an initially expanding homogeneous sphere in pure Hubble flow. Results of a number of simulations are summarized in Table 1.

The dissipationless cold start simulations agree with those of previous workers: $v(r) \equiv [GM(r)/r]^{1/2}$ peaks at about 15 kpc and then falls off, unlike observed spiral galaxy rotation curves. As might be expected from the analytic model discussed in § II, baryonic infall moves the peak in $v(r)$ inward and accentuates its decline at larger radii, which agrees even less well with observations.

The hot start results are more interesting. The dashed line in Figure 3 shows $v(r)$ resulting from a dissipationless simulation. It resembles an isothermal sphere with a large core radius of about 45 kpc, reflecting the large initial kinetic energy. A simulation with the same initial conditions but including baryonic dissipation is shown by the solid curve in the figure. Owing to the large merging cross section, about half of the baryonic mass ends up merged into a "fat baryon" at a radius of about 12 kpc, which is of course unrealistic. Nevertheless, the overall shape of the rotation curve ought to approximate fairly well the dynamical effects of baryonic infall, at least at radii well beyond the fat baryon. Dark matter is pulled in toward the center, and the rotation curve is rather like those of real galaxies.

The dotted curve in Figure 3 compares the hot start model with an analytic version of the same calculation, as described in § II. The analytic version starts with the final mass distribution from the dissipationless N-body simulation (dashed curve) and brings the baryons to a final spherical distribution with the same $M_b(r)$ as in the dissipational N-body simulation. The resulting rotation curve is in rough agreement with that from the dissipational N-body simulation, although the analytic calculation somewhat overestimates the pulling in of the dark matter compared to the N-body simulation. This occurs because of the assumption in the analytic calculation that the baryonic infall is spherically symmetric and because the infall takes place *after* rather than *simultaneously* with dynamical relaxation, as in the N-body simulation. Note that baryonic infall does not affect the outer rotation curve, which declines with radius in both simulations. The simulations are probably not to be trusted at large radii because of edge effects. On the other hand, the behavior at large radii cannot yet be checked directly, because the observations of rotation curves of galaxies do not extend out this far.

In the Hubble start simulations, the initially purely radial velocity is somewhat randomized as subclusters form while the system expands and contracts before violent relaxation. The resulting dissipationless simulations thus have fairly large core radii, about 15 kpc. In the simulations that include baryonic infall, dark matter is pulled in toward the center, producing relatively flat rotation curves that resemble those of real galaxies. Figure 4 shows the results of such a simulation. As before, the formation of a "fat baryon" makes the inner part of the simulation unrealistic. If the protogalaxy had acquired more internal kinetic energy—through effects not included in our simulations, such as a spherical collapse, tides, or the gravitational interactions of preexisting internal subcondensations—then the core radius of the dissipationless simulation would have been larger, and the intermediate part

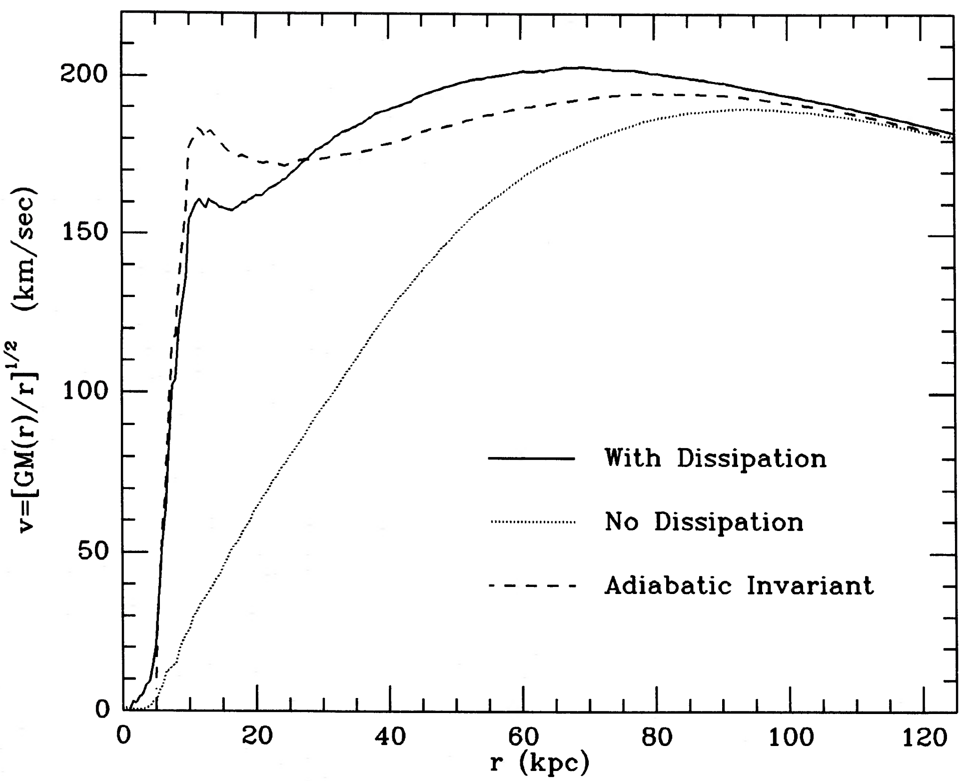

FIG. 3.—Rotation velocity, $v = (M/r)^{1/2}$, vs. r for a "hot start" N-body simulation (4th row of Table 1). *Dashed line*, rotation curve for the dissipationless N-body simulation; *solid line*, curve for the dissipational simulation. Dotted line obtained by applying the method of § II (see text).

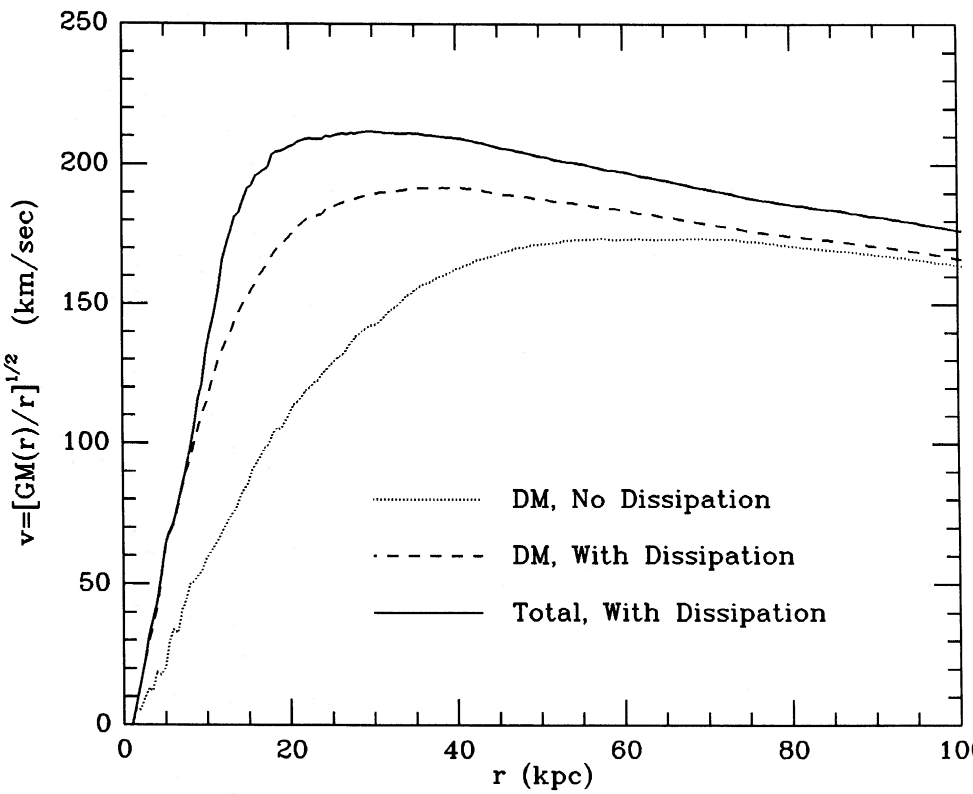

FIG. 4.—Results from a " Hubble start" N-body simulation (8th row of Table 1). *Dotted curve*, $[M_{\rm DM}(r)/r]^{1/2}$ from the dissipationless simulation; *dashed curve*, corresponding result from the dissipational simulation. *Solid curve*, rotation curve $v = (M/r)^{1/2}$ from the dissipational simulation.

TABLE 1

N-Body Simulations

					No Dissipation			Dissipation					
F	ϵ (kpc)	Q	λ	R_m/R_i	a_{DM} (kpc)	v_m	$v(20)$ (km s^{-1})	a_{DM} (kpc)	v_m	$v(20)$ (km s^{-1})	$M_b(20)/M_b$ tot	$(M_{DM}^{diss}/M_{DM}^{no\ diss})\|_{20}$	$(M_b^{diss}/M_{DM}^{diss})\|_{20}$
Cold start:													
0.1	0.5	0.02	0.07	1	4.5	330	325	5.2	340	330	0.92	1.1	0.19
Hot start:													
0.1	0.5	0.5	0	1	33	180	80	23	200	180	0.65	2.3	1.2
0.1	0.5	0.5	0.07	1	32	190	90[a]	17	200	180	0.64	3.0	1.00
0.1	5.0	0.5	0.07	1	40	180	70[a]	16	190	165	0.61	3.4	1.04
0.2	0.5	0.5	0.07	1	32	190	75	13	390[a]	240	0.85	4.0	2.0
0.1	0.5	0.5	0.14	1	26	185	100	15	195	180	0.55	2.2	0.67
Hubble start:													
0.1	0.5	0.6	0.07	2.5	17	180	140	16	200	180	0.46	1.3	0.45
0.1	2.5	0.6	0.07	2.5	22	180	115	12	210	210	0.56	2.4	0.40
0.05	0.5	0.6	0.07	2.5	21	180	115	16	190	160	0.24	1.7	0.16
0.3	0.5	0.6	0.07	2.5	12	185	160	4	400[a]	290	0.82	1.6	1.7
0.1	0.5	0.73	0.07	3.6	18	180	140	12	200	200	0.60	1.5	0.5

Note.—F, fraction of total mass in baryons; ϵ, softening parameter; Q, (total kinetic energy)/|total potential energy| initially; λ, dimensionless angular momentum parameter $\lambda = J|E|^{1/2}G^{-1}M^{-5/2}$; R_m/R_i, (maximum radius)/(initial radius); a_{DM}, dark matter characteristic radius, defined by $v_{DM}(a_{DM}) = 0.67v_{DM,max}$, corresponding to $\rho_{DM}(a_{DM}) = 0.5\rho_{DM}(0)$ for an isothermal sphere. Here $v_{DM}(r) = [GM_{DM}(r)/r]^{1/2}$; v_m, maximum of $v(r) = [GM(r)/r]^{1/2}$, where $M(r)$ = total mass interior to radius r; $v(20)$, $v(r)$ at 20 kpc; $M_b(20)/M_b$ tot, (baryonic mass interior to 20 kpc, with dissipation)/(total baryonic mass); $(M_{DM}^{diss}/M_{DM}^{no\ diss})|_{20}$, (DM mass inside 20 kpc, with dissipation)/(DM mass inside 20 kpc, without dissipation); $(M_b^{diss}/M_{DM}^{diss})|_{20}$ (baryonic mass inside 20 kpc, with dissipation)/(DM mass inside 20 kpc, with dissipation).

[a] Error approximately 15%. (Other statistical errors are less than 10%.)

of the rotation curve from the dissipational simulation would have been flatter or still rising. This would have been more like the analytic calculations graphed in Figure 1 and would agree even better with real galaxies. This simulation illustrates how important it is to understand the clustering properties of the dark matter in the absence of dissipation and, in particular, how large and diffuse the core radii of dissipationless halos would be. Estimates of the range of internal kinetic energy to be expected in real protogalaxies can perhaps be obtained from N-body simulations of the evolution of a larger region containing several galaxies, starting from an appropriate initial fluctuation spectrum.

Table 1 summarizes various properties of these simulations and compares results for various cases. One of the quantities shown is $M_b(20)/M_b^{\rm tot}$, which is roughly the fraction of baryons that ultimately wind up within the optical radius of the galaxy. This is a measure of the efficiency of baryonic infall and is typically around 60% for most models. The corresponding figure for no dissipation is about 2%–3%. Another quantity shown is $M_{\rm DM}^{\rm diss}/M_{\rm DM}^{\rm no\ diss}|_{20}$, which is the mass ratio of dark matter for the dissipational and dissipationless cases within roughly the optical radius (20 kpc). This quantity is a measure of the pulling in of the dark matter by the baryons. For the hot start case that yields the flattest, best fitting rotation curve, this ratio is around three, not far different from the value of two to three that is obtained at the analogous radii for the best fitting analytic model of § II.

The table also shows the final ratio of baryonic to dark matter within 20 kpc. This ratio varies considerably for the various cases but is close to unity for the best fitting hot start model. This agrees well with real galaxies, for which the mass in baryons approximates the mass in dark matter within the optical radius (e.g., Burstein *et al.* 1982).

Most of the N-body simulations were run with the dimensionless angular momentum parameter $\lambda \equiv J|E|^{1/2}G^{-1}M^{-5/2}$ having an initial value $\lambda = 0.07$, as obtained in numerical simulations (Peebles 1971; Efstathiou and Jones 1979). Here E is the total energy of the system, and the angular momentum is imposed by rigid-body rotation. Table 1 shows that the effects of varying the initial value of λ are as one might expect: the extent of baryonic infall decreases as λ increases. This is analogous to varying b in the analytic models of § II.

Table 1 also shows that the simulations are very sensitive to the parameter F, the ratio of baryonic to total mass. This is also in agreement with the analytic results and is discussed further in the next section.

IV. DISCUSSION

Two recent papers (Burstein and Rubin 1985; Bahcall and Casertano 1985) have called attention to the fact that galactic rotation curves are remarkably flat and featureless. As Figure 1 illustrates, this behavior is not an inevitable feature of galaxy models with two different kinds of mass: witness the rising rotation curves and curves with local maxima illustrated there. The above authors have speculated whether there might exist some higher, controlling process that regulates the distribution of both mass components, merging them in such a way that no discontinuities remain, or whether there may even be just one kind of matter—baryonic—that is in some regions visible and in others not.

The present numerical experiments shed some new light on this question. They suggest a plausible scenario involving dissipational infall that can lead naturally to flat rotation curves if two conditions are satisfied. The first is the existence of halos with intrinsically large, diffuse cores and flat outer rotation curves in the absence of dissipation. These characteristics can both be achieved, we have seen, if substantial internal kinetic energy exists at the epoch of maximum expansion, and reasonable mechanisms for generating this energy are known. The second condition calls for a balance between the mass fraction in baryons and the degree to which they fall in, which are controlled by the parameters F and λ respectively. There are significant observational constraints on F that place it near 0.1 in rough order of magnitude (Blumenthal *et al.* 1984). Likewise, theoretical estimates place λ near 0.07, as noted above. Interestingly, with large-core halos, these values yield just the right balance between baryon mass and infall to produce fairly flat rotation curves in our simulations. The compression of the dark matter by baryonic infall further serves to smooth out any discontinuities in the rotation curve that might have resulted from infall in a purely rigid halo. It is not known whether the above scenario for producing flat rotation curves with dissipative infall is unique, but it does have the advantage that each of its key elements is either plausible or supported by independent arguments.

This picture is encouraging but not yet complete. For example, Burstein and Rubin (1985) have noted that the rotation curves of galaxies divide into several distinct families. The mass distribution has a similar form within a family and a substantially different form from those of other families. Remarkably, there seems to be little correspondence between the Hubble type or visible baryonic mass distribution and the form family. The origin of these form families of rotation curves is not yet understood in the dissipative infall picture of galaxy formation.

V. CONCLUSIONS

The principal conclusion of this paper is that dark-matter halos of galaxies are "squeezable" during formation via the dissipative infall of baryons. The resultant inner density profiles are strongly perturbed, with smaller core radii and higher central densities than would have been obtained without dissipation. As a result, it is unlikely that halos today have strictly isothermal profiles. Halo compressibility also means that the final collapse radii and radial distribution of the baryons cannot be computed with the rigid-halo approximation.

Baryonic infall increases rotation velocity in the inner regions and is therefore incapable of flattening out an initial rotation curve that falls too steeply; indeed, it merely worsens the effect. A final flat curve therefore requires a fairly flat curve in the absence of dissipation. This occurs naturally in models with substantial internal kinetic energy at maximum expansion. Models of this type coincidentally develop large, diffuse cores, consistent with the conclusion that today's small cores are the result of substantial compression. The origin of the necessary internal kinetic energy is still unclear, but there are at least three possibilities: subclustering, aspheric collapse, and tidally induced internal streaming.

Rotation curves flat enough to match the observations are obtained only with a restricted range of infall parameters. For models with large, diffuse cores, a good match is obtained if the baryonic fraction F and the ratio of exponential disk scale to infall radius b/R both lie between roughly 0.05 and 0.2. This general range is in good agreement with limits set by observational data and the tidal torque theory of angular momentum. A scenario based on dissipative infall with large, diffuse halos in the absence of dissipation and with F and b close to their conventional values thus provides a plausible explanation for flat rotation curves in two-component mass models for galaxies.

There are several ways in which the present models need to be improved. Most important is a realistic final baryonic density distribution, without which the details of the inner rotation curve remain unconvincing. A larger expansion factor is also needed in the expanding Hubble case to give subclustering a fairer chance to develop. Subclustering also depends on the initial density fluctuation spectrum, which in the present models is simply Poisson white noise. Other cases, such as cold dark matter, need to be investigated. Finally, the present calculations model only the volume occupied by the protogalaxy itself. Ideally this volume should be embedded self-consistently within a larger volume of the expanding universe. It is hoped to explore some of these refinements in future work.

This paper was partly inspired by conversations with Dr. David Burstein and Dr. S. J. Aarseth. We also thank Dr. Aarseth for instructing us in the use of his N-body code. After doing the calculations reported here, we learned of related work from Dr. James Gunn, who told us of calculations by his student Barbara Ryden (Ryden and Gunn 1984) that resemble those reported in § II, and from Dr. Joshua Barnes, who has independently done some similar N-body calculations. We thank them for sharing their results in advance of publication. Our work has been supported by NSF grants PHY84-15444 and AST 82-11551, by a UCSC faculty research grant, and by Department of Energy contract DE-AC02-ER03230 at Brandeis. In addition, we are extremely grateful to Professor James Bensinger for allowing us to use the High Energy Physics VAX at Brandeis and to Professor Karen McNally for allowing us to use the Seismology VAX at Santa Cruz for the N-body simulations.

REFERENCES

Aarseth, S. J. 1979, in *Instabilities in Dynamical Systems*, ed. V. Szebehely (Dordrecht: Reidel), p. 69.
Aarseth, S. J., and Fall, S. M. 1980, *Ap. J.*, **236**, 43.
Bahcall, J. N., and Casertano, S. 1985, preprint.
Bahcall, J. N., Schmidt, M. A., and Soneira, R. M. 1982, *Ap. J.* (*Letters*), **258**, L23.
Blumenthal, G. R., Faber, S. M., Primack, J. R., and Rees, M. J. 1984, *Nature*, **311**, p. 527.
Bosma, A. 1978, Ph.D. Thesis, Groningen.
Burstein, D., and Rubin, V. C. 1985, preprint.
Burstein, D., Rubin, V. C., Thonnard, N., and Ford, W. K. 1982, *Ap. J.*, **253**, 70.
Caldwell, J. A. R., and Ostriker, J. P. 1982, *Ap. J.*, **251**, 61.
Dekel, A., Kowitt, M., and Shaham, J. 1981, *Ap. J.*, **250**, 561.
Efstathiou, G., and Jones, B. J. T. 1979, *M.N.R.A.S.*, **186**, 133.
Faber, S. M. 1982, in *Astrophysical Cosmology: Proceedings of the Vatican Study Week on Cosmology and Fundamental Physics*, ed. H. A. Brück, G. V. Coyne, and M. S. Longair (Rome: Specola Vaticana), p. 219.
Fall, S. M., and Efstathiou, G. 1980, *M.N.R.A.S.*, **193**, 189.
Gott, J. R. 1973, *Ap. J.*, **186**, 481.
———. 1975, *Ap. J.*, **201**, 296.
Gould, R. J., and Thakur, R. K. 1970, *Ann. Phys.*, **61**, 351.
Gunn, J. E. 1977, *Ap. J.*, **218**, 592.
———. 1982, in *Astrophysical Cosmology: Proceedings of the Vatican Study Week on Cosmology and Fundamental Physics*, ed. H. A. Brück, G. V. Coyne, and M. S. Longair (Rome: Specola Vaticana), p. 233.
Gunn, J. E., and Gott, J. R. 1972, *Ap. J.*, **176**, 1.
Jones, B. J. T., and Efstathiou, G. 1979, *M.N.R.A.S.*, **189**, 27.
Lynden-Bell, D. 1967, *M.N.R.A.S.*, **136**, 101.
Peebles, P. J. E. 1971, *Astr. Ap.*, **11**, 377.
Pryor, C., and Lecar, M. 1983, *Ap. J.*, **269**, 513.
Rubin, V. C. 1982, *Science*, **220**, 1339.
Rubin, V. C., Ford, W. K., and Thonnard, N. 1980, *Ap. J.*, **238**, 471.
Ryden, B., and Gunn, J. E. 1984, *Bul. AAS*, **16**, 487.
Shu, F. H. 1978, *Ap. J.*, **225**, 83.
Smith, B. F., and Miller, R. H. 1985, preprint.
Steigman, G., Sarazin, C. L., Quintana, H., and Faulkner, J. 1978, *A.J.*, **83**, 1050.
White, S. D. M., and Rees, M. J. 1978, *M.N.R.A.S.*, **183**, 341.
Zel'dovich, Ya. B., Klypin, A. A., Khlopov, M. Yu., and Chechetkin, V. M. 1980, *Soviet J. Nucl. Phys.*, **31**, 664.

GEORGE R. BLUMENTHAL and SANDRA M. FABER: Lick Observatory, Board of Studies in Astronomy and Astrophysics, University of California, Santa Cruz, CA 95064

RICARDO FLORES: Department of Physics, Brandeis University, Waltham, MA 02254

JOEL R. PRIMACK: Board of Studies in Physics, University of California, Santa Cruz, CA 95064